



Fabrication and characterization of Co-Mn-Al Heusler-type thin film

著者	安藤 康夫
journal or publication title	Journal of applied physics
volume	97
number	10
page range	10C913-1-10C913-3
year	2005
URL	http://hdl.handle.net/10097/35853

doi: 10.1063/1.1852329

Fabrication and characterization of Co–Mn–Al Heusler-type thin film

H. Kubota^{a)}

Nanoelectronics Research Institute, National Institute of Advanced Industrial Science and Technology (AIST), Umezono 1-1-1, Tsukuba 305-8568, Japan

J. Nakata, M. Oogane, Y. Ando, H. Kato, A. Sakuma, and T. Miyazaki

Department of Applied Physics, Graduate School of Engineering, Tohoku University, Aoba-yama 05, Aramaki, Aoba-ku, Sendai 980-8579, Japan

(Presented on 9 November 2004; published online 5 May 2005)

Co–Mn–Al thin films were prepared using ultrahigh-vacuum magnetron sputtering on thermally oxidized silicon substrates at various substrate temperatures. Composition, crystal structure, magnetic property, and surface roughness of the films were investigated. The film prepared at a substrate temperature (T_s) of around 300 °C had Co_2MnAl $B2$ structure, revealing partial disorder between Mn and Al sites. Magnetization exhibited a maximum and coercive field exhibited a minimum around $T_s=300$ °C. Surface roughness increased with the substrate temperature. The film prepared at a substrate temperature of 300 °C was applied to a bottom electrode of a magnetic tunnel junction, thereby creating a large tunnel magnetoresistance. © 2005 American Institute of Physics. [DOI: 10.1063/1.1852329]

Some Heusler alloys, such as NiMnSb^1 or Co_2MnGe^2 , have been predicted to be half-metallic ferromagnetic (HMF), meaning that they have large asymmetry of density of states at Fermi energy (E_F). The HMF allows very large magnetoresistance in the magnetic tunnel junction (MTJ), which is necessary for use in high capacity magnetic random access memories³ (MRAMs) or highly sensitive magnetic sensors.⁴ Ishida *et al.* predicted theoretically that $\text{Co}_2\text{Mn}(\text{Al}_{1-x}\text{Si}_x)$ alloy with $L2_1$ structure can be HMF at $x > 0.4$.⁵ Experimentally, film growth of some kinds of Heusler alloy^{6,7} or magnetoresistive property of the single films^{8,9} was studied, but only a few experiments on tunnel magnetoresistance have been reported on MTJs using Heusler alloy.^{10,11} Quite recently, large tunnel magnetoresistance has been obtained successfully in MTJs using Co_2MnSi (33% at RT, 86% at 10 K) independently by Kämmerer *et al.*¹² and in Co_2MnAl (40% at RT and 65% at 10 K) by our group.¹³ In the present study, we characterized Co–Mn–Al thin films that had been prepared by sputtering at various substrate temperatures (T_s). Composition, crystal structure, and magnetic properties of the Co–Mn–Al thin films changed remarkably with T_s . Optimization of these properties is necessary to achieve large magnetoresistance in MTJ with Co_2MnAl Heusler alloy.

Co–Mn–Al (300 nm) films and Cr(10 nm)/Co–Mn–Al(20 nm) films were prepared on thermally oxidized Si substrates using dc and rf magnetron sputtering. The Ar pressures during sputtering were about 0.1 Pa. A sputtering target used for Co–Mn–Al layer had a stoichiometric Co_2MnAl (Co:Mn:Al=50:25:25, 99.9%) composition that was prepared by Kojundo Chemical Lab. Co., Ltd. Substrate temperature for the Cr buffer layers was fixed at 200 °C. Substrate temperatures for the Co–Mn–Al films were varied

from ambient temperature to 600 °C. X-ray diffraction method with in-plane geometry and atomic force microscopy confirmed the crystal structure and surface roughness of the Co–Mn–Al thin films, respectively. Film compositions were examined using energy dispersion spectroscopy (EDS). One thick Co–Mn–Al film was examined by inductively coupled plasma (ICP) analysis. It is necessary to calibrate EDS results using samples with an accurate composition. In this experiment, compositions of films with various substrate temperatures obtained by EDS analysis (sample thickness with about 300 nm) were corrected using the composition obtained by the ICP analysis with high accuracy (sample thickness with about 500 nm, $T_s=300$ °C). We measured magnetization curves using a vibrating sample magnetometer and a superconducting quantum interference device (SQUID) magnetometer.

Figure 1 shows the x-ray diffraction patterns of 300

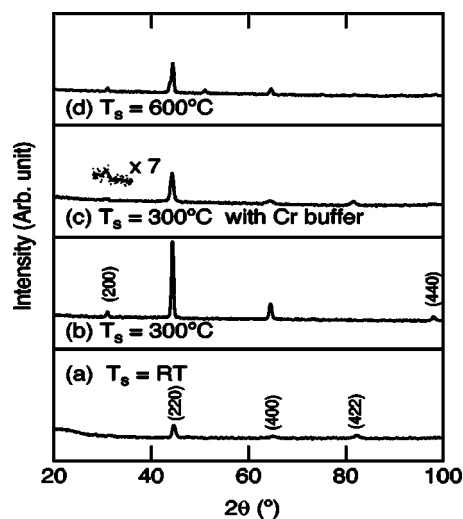


FIG. 1. X-ray diffraction patterns of Co–Mn–Al thin films prepared at various substrate temperatures.

^{a)}Author to whom correspondence should be addressed; electronic mail: hit-kubota@aist.go.jp

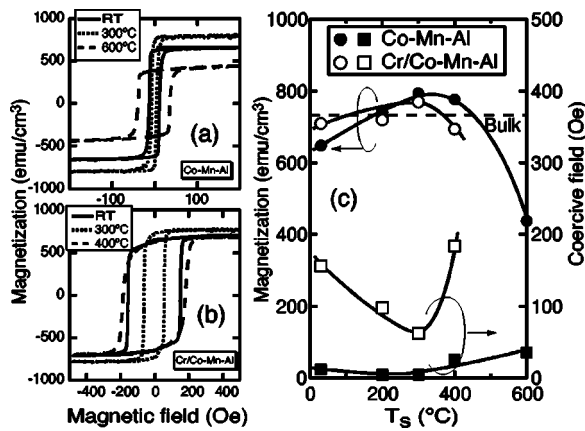


FIG. 2. Magnetic properties of Co-Mn-Al single films and Cr/Co-Mn-Al films prepared at various substrate temperatures.

-nm-thick Co-Mn-Al single films grown on the substrates [Figs. 1(a), 1(b), and 1(d)] and 20-nm-thick Co-Mn-Al thin films with 10-nm-thick Cr buffer layers [Fig. 1(c)] prepared at various substrate temperatures. The thick film grown at RT [Fig. 1(a)] showed small peaks of (220), (400), and (422) crystal planes, but no distinct peak of the (200) plane, resulting in A2 structure with a large degree of disorder among Co, Mn, and Al sites. A broad peak at $2\theta < 30^\circ$ was caused by an amorphous portion in the film. The (200) peak of the B2 structure was observed clearly in the profile of the film grown at 300 °C [Fig. 1(b)]. The ratio of peak intensities of the (200) and (220) planes agreed with that of the powder pattern of the B2 structure. No other peaks were observed to originate in pure Co or other alloys. The 20-nm-thick Co-Mn-Al film grown at $T_s = 300^\circ\text{C}$ on the Cr buffer layer also showed the B2 structure of Co_2MnAl . The peak of the (200) plane is observable in Fig. 1(c). A film grown at 600 °C [Fig. 1(d)] showed additional peaks at 51° , 75° , and 91° . Those peaks originated in a fcc phase (unknown) other than the B2 structure.

Figures 2(a) and 2(b) show the magnetization curves of the Co-Mn-Al (30 nm) single films and the Cr(10 nm)/Co-Mn-Al(20 nm) film. Magnetizations of the thick films increased steeply and saturated at low magnetic fields. This behavior agreed well with that of the bulk case. Coercive fields in the Cr(10 nm)/Co-Mn-Al(20 nm) film were larger than those of the Co-Mn-Al (30 nm) single film at the same T_s . In the secondary-ion-mass spectroscopy (SIMS) depth profile, Cr intensity was negligible in the volume of the Co-Mn-Al layer. At the bottom of the Co-Mn-Al layer, there was a tail of the Cr signal into the Co-Mn-Al layer, but the precise thickness of the interdiffusion layer was not evaluated. To clarify the origin of the large coercive field, further investigation is necessary to elucidate the intermixing layer at the interface between the Cr and Co-Mn-Al layers. In both films, magnetization showed a maximum and a coercive field showed a minimum around $T_s = 300^\circ\text{C}$. The decrease of magnetizations and increase of coercive fields corresponded to structural degradation at high substrate temperatures. The crystal structure and the magnetic properties suggested that the Co-Mn-Al film quality became comparable to that of bulk around $T_s = 300^\circ\text{C}$. How-

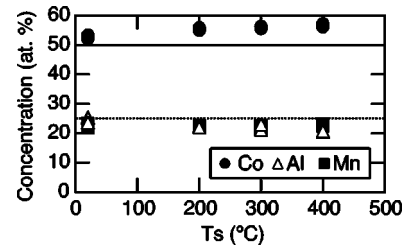


FIG. 3. Composition of Co-Mn-Al films as a function of substrate temperature.

ever, the maximum value of magnetization exceeded the bulk value. Large magnetizations were related to film composition. Figure 3 depicts the film composition as a function of substrate temperature. Composition of the alloy film prepared at $T_s = \text{RT}$ showed approximate stoichiometry (Co:Mn:Al=50:25:25). Co concentration increased with increasing T_s . Correspondingly, Mn and Al concentrations decreased slightly. The composition of the alloy film prepared at $T_s = 300^\circ\text{C}$ was about Co 56 at. %, Mn 22 at. %, and Al 22 at. %. Large magnetization is attributable to the excess amount of Co atoms in the thin films.

Resistivity is very sensitive to film structure: defects, grain, and atomic disorder. Figure 4 shows the resistivity of 50-nm-thick Co-Mn-Al single films. Resistivity decreased with increasing T_s and showed a minimum around $T_s = 300^\circ\text{C}$. The minimum value was about $220\ \mu\Omega\text{cm}$, which is much higher than those of usual metal films. In our previous study,¹⁴ bulk Co_2MnAl alloy also showed a high residual resistivity of about $200\ \mu\Omega\text{cm}$. Its temperature dependence was very weak because Co_2MnAl has a partial disorder between Mn and Al sites. Structural features, such as defect density, grain size, and the degree of disorder, affecting film resistivity closely approximated those of bulk at $T_s = 300^\circ\text{C}$. Consequently, the main component of the Co-Mn-Al films prepared at $T_s = 300^\circ\text{C}$ was Co_2MnAl with the B2 structure.

Finally, this study examined the effect of substrate temperature on surface roughness. Figure 5 shows the average roughness of the Cr(10 nm) buffer surface and Cr(10 nm)/Co-Mn-Al(20 nm) double layer as a function of substrate temperature. The insets are atomic force-microscopy (AFM) images obtained on the surface of a Cr (10 nm) buffer layer grown at 200 °C (left) and a Co-Mn-Al (20 nm) film grown at 300 °C on a Cr buffer layer grown at 200 °C (right). The scan area was $500 \times 500\ \text{nm}^2$. In the images of the Cr surface, the fine structure of grains was observed at $T_s = 200^\circ\text{C}$ and the roughness was sufficiently small as a buffer layer. The roughness increased rap-

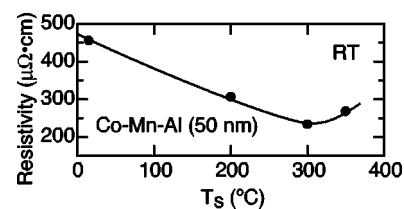


FIG. 4. Resistivity of Co-Mn-Al films as a function of substrate temperature.

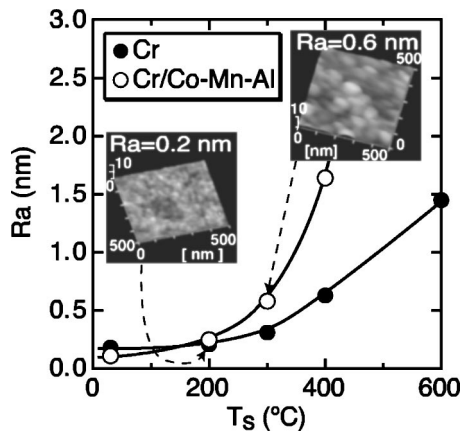


FIG. 5. Surface roughness of Co–Mn–Al films as a function of substrate temperature. Insets show AFM images of the Cr(10 nm) buffer surface and Cr(10 nm)/Co₂MnAl(20 nm) surface.

idly at $T_s > 300$ °C. The roughness of the Cr(10 nm)/Co–Mn–Al(20 nm) double layer also increased with increasing T_s . In these films, Cr buffers were grown at 200 °C. The AFM image of the double layer with $T_s = 300$ °C showed grain growth of the Co–Mn–Al film, where roughness (R_a) was about 0.6 nm. The MTJs using the Cr(10 nm)/Co–Mn–Al(20 nm) bottom electrode ($T_s = 200$ °C for Cr and $T_s = 300$ °C for Co–Mn–Al) with an Al–O insulating layer and a Co₇₅Fe₂₅(4 nm)/Ir–Mn(10 nm) top electrode showed large tunnel magnetoresistance (TMR) ratios of about 40% at RT and 65% at 10 K.¹³ Those ratios were much larger than the previous results recorded for Heusler-based MTJs.^{10,11} The larger TMR ratio is inferred to result from the good crystallinity and smooth surface of the Heusler-based bottom electrode.

In summary, we have investigated the effect of substrate temperature on structural, magnetic, and electrical properties of Co–Mn–Al films. At a substrate temperature of 300 °C, the Co–Mn–Al film properties became comparable to that of bulk. The thin Co–Mn–Al film grown on the Cr buffer layer had a sufficiently smooth surface to allow its application as a bottom electrode in MTJ.

This study was supported by the IT-Program of the Research Revolution 2002 (RR2002) “Development of Universal Low-Power Spin Memory” and a Grant-in-Aid for Scientific Research from the Ministry of Education, Culture, Sports, Science and Technology of Japan, CREST of Japan Science and Technology (JST).

- ¹R. A. de Groot, F. M. Mueller, P. G. van Engen, and K. H. J. Buschow, *Phys. Rev. Lett.* **50**, 2024 (1983).
- ²S. Ishida, T. Masaki, S. Fujii, and S. Asano, *Physica B* **245**, 1 (1998).
- ³M. Durlam *et al.*, *Tech. Dig. - Int. Electron Devices Meet.* **2003**, 34.6.1 (2003).
- ⁴S. Bae, J. H. Judy, I.-F. Tsu, and M. Davis, *J. Appl. Phys.* **94**, 7636 (2003).
- ⁵S. Ishida, S. Fujii, S. Kashiwagi, and S. Asano, *J. Phys. Soc. Jpn.* **64**, 2152 (1995).
- ⁶W. Van Roy, M. Wojcik, E. Jedryka, S. Nadolski, D. Jalabert, B. Brijs, G. Borghs, and J. De Boeck, *Appl. Phys. Lett.* **83**, 4214 (2003).
- ⁷P. Turban, S. Andrieu, B. Kierren, C. Teodorescu, and A. Traverse, *Phys. Rev. B* **65**, 134417 (2002).
- ⁸B. Heinrich, G. Woltersdorf, R. Urban, O. Mosendz, Simon Fraser, G. Schmidt, P. Bach, and L. Molenkamp, *J. Appl. Phys.* **95**, 7462 (2004).
- ⁹T. Ambrose, J. J. Krebs, and G. A. Prinz, *J. Appl. Phys.* **87**, 5463 (2000).
- ¹⁰C. T. Tanaka, J. Nowak, and J. S. Moodera, *J. Appl. Phys.* **81**, 5515 (1997).
- ¹¹K. Inomata, N. Tezuka, S. Okumura, H. Kurebayashi, and A. Hirohata, *J. Appl. Phys.* **95**, 7234 (2004).
- ¹²S. Kämmerer, A. Thomas, A. Hütten, and G. Reiss, *Appl. Phys. Lett.* **85**, 79 (2004).
- ¹³H. Kubota, J. Nakata, M. Oogane, Y. Ando, A. Sakuma, and T. Miyazaki, *Jpn. J. Appl. Phys., Part 2* **43**, L985 (2004).
- ¹⁴T. Endo, H. Kubota, and T. Miyazaki, *J. Magn. Soc. Jpn.* **23**, 1129 (1999).